Transport coefficients of soft repulsive particle fluids

2008 J. Phys.: Condens. Matter 20 115102

(http://iopscience.iop.org/0953-8984/20/11/115102)

J. Phys.: Condens. Matter **20** (2008) 115102 (8pp) doi:10.1088/0953-8984/20/11/115102

Transport coefficients of soft repulsive particle fluids

D M Heyes[1] **and A C Brańka**[2]

[1] Division of Chemical Sciences, Faculty of Health and Medical Sciences, University of Surrey, Guildford GU2 7XH, UK
[2] Institute of Molecular Physics, Polish Academy of Sciences, Smoluchowskiego 17, 60-179 Poznań, Poland

E-mail: d.heyes@surrey.ac.uk and branka@ifmpan.poznan.pl

Received 5 November 2007, in final form 9 January 2008
Published 20 February 2008
Online at stacks.iop.org/JPhysCM/20/115102

Abstract

Molecular dynamics computer simulation has been used to compute the self-diffusion coefficient, D, and shear viscosity, η_s, of soft-sphere fluids, in which the particles interact through the soft-sphere pair potential, $\phi(r) = \epsilon(\sigma/r)^n$, where n measures the steepness or stiffness of the potential, ϵ and σ are a characteristic energy and distance, respectively. The simulations were carried out on monodisperse systems for a range of n values from the hard-sphere ($n \to \infty$) limit down to $n = 4$ over a range of densities. An ideal glass transition value was estimated from the limit where D and $\eta_s^{-1} \to 0$ for each value of n. Nucleation of the crystalline phase was found to intervene prior to the formation of the glass itself, as has been found previously for hard spheres (i.e. $n \to \infty$). With increasing softness the glass transition moves further within the solid part of the phase diagram, as predicted by Cardenas and Tosi (2005 *Phys. Lett.* A **336** 423), although the volume fractions at the glass transition estimated by the current procedure here are systematically lower than the predictions of that study.

S Supplementary data are available from stacks.iop.org/JPhysCM/20/115102

1. Introduction

The dense packing of soft particles is a process that occurs widely in nature and in many industrial manufacturing processes. These 'jammed' or 'glassy' states can be created by cooling a thermalized system (e.g. by vibration of the bed for powders, or by Brownian motion for colloidal systems) at constant pressure, or by compressing it isothermally (e.g. see [1]). The temperature route to the jammed state is complicated by the fact that both the temperature and density usually are allowed to change simultaneously, which requires a decoupling of the effects of these two parameters (e.g. see [2] for a discussion of this subject). In contrast, the application of pressure under isothermal conditions solely affects the density. Cooling is much easy to achieve in experiment, whereas in molecular simulation the two processes can be introduced with comparable ease, and it is the compression route towards the glassy state that we follow here.

Hard spheres undergo a fluid-to-crystalline phase transition above a critical density which is driven purely by configurational entropy, while for soft particle enthalpic factors are important as well. In this study the compression of model fluids into the metastable fluid and solid parts of their phase diagrams are undergone using molecular dynamics simulations. The inverse power or soft-sphere potential is a convenient representation of a particle with variable softness,

$$\phi(r) = \epsilon \left(\frac{\sigma}{r}\right)^n, \tag{1}$$

where r is the separation between two particles, σ is a nominal particle diameter, ϵ sets the energy scale and n is a parameter that determines the potential steepness (the softness is $\varepsilon \sim n^{-1}$). The soft-sphere potential provides a continuous path from hard spheres ($n \to \infty$) to $n > 3$ which covers a wide range of softnesses and particle types. The thermodynamic properties of the soft-sphere system can be expressed in terms of a reduced parameter, $\tilde{\rho} = \rho(k_B T/\epsilon)^{-3/n}$ where ρ is the reduced number density ($= N\sigma^3/V$, for N particles in volume V), k_B is Boltzmann's constant and T is the temperature. Therefore the equilibrium part of the phase diagram can be expressed in terms of the density dependence along a single value of the reduced temperature, $T^* = k_B T/\epsilon$, usually taking $T^* = 1$ for convenience. The solid–fluid phase boundary as a function of n is known accurately in the range $0 \leqslant n^{-1} \leqslant 0.32$ from Gibbs–Duhem integration [3, 4].

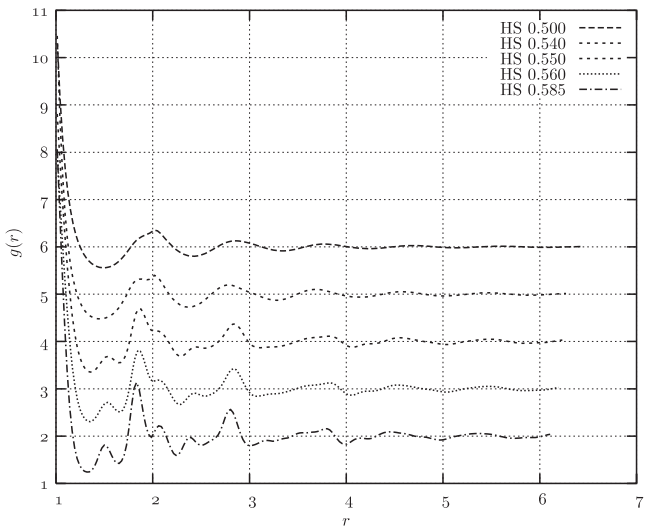

Figure 1. Radial distribution of the hard-sphere fluid at various packing fractions, given on the figure for $N = 2048$ systems. The selected functions are displaced by units of 1 systematically from each other to help clarify the trends with density. The system nucleates at ca. $\zeta = 0.545$.

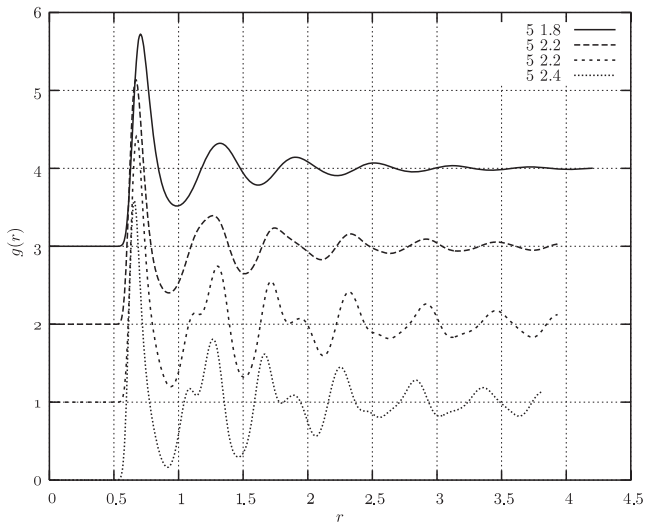

Figure 2. Radial distribution of the r^{-5} fluid at various packing fractions, given on the figure, otherwise as for figure 1. The number of particles in the simulation cell was 2048. The system nucleated at $\zeta = 2.2$. The two radial distribution functions shown at this packing fraction are one prior to and one after nucleation at $\zeta = 2.2$.

Molecular dynamics, MD, simulations were carried out for assemblies of particles interacting via the soft-sphere potential of equation (1), for microcanonical and constant temperature simulations, the latter by velocity rescaling. Steepness parameter values down to $n = 4$ were considered. The limiting case of $n \to \infty$ is the hard-sphere fluid, which requires a different 'event-driven' procedure to follow its dynamics. The self-diffusion coefficients of the hard-sphere limit are known well from previous studies (e.g. see [5]). Most of the simulations were carried out with $N = 2048$ particles, at a reduced temperature, $k_B T/\epsilon = 1$ (see [6] for further details). All quantities are given in terms of the basic units of σ, ϵ and m, the mass of a particle. The definitions for the computed quantities are standard and may be found, for example, in [7, 8]. The transport coefficients were obtained from the appropriate Green–Kubo formula. The density is expressed here in terms of the nominal packing fraction, $\zeta = \pi N \sigma^3/6V$. The density of the system was increased in stages, and the time-averaged quantities collected at each fixed density. The fluid–solid coexistence densities, ζ_f and ζ_s for the soft-sphere fluid at the various n are already in the literature, [4]. On compression in the fluid–solid metastable region of the phase diagram, the system nucleates before it reaches the glass transition. The nucleation packing fraction, ζ_n, is readily identified by a sharp drop in the value of D, which occurs typically after D has decreased to a value of ca. 0.01. The appearance of crystalline features in the radial distribution function is also another signature that crystalline or polycrystalline nucleation had taken place. In fact, most molecular simulations of glass formation are carried out using binary mixtures to frustrate nucleation [9]. There is therefore a question as to whether simple liquids have a glass transition, owing to the difficulty in bypassing crystallization on cooling or compressing these liquids by molecular dynamics.

Since the attainment of the glassy state and the definition of the glassy state depend on experimental timescales it is natural to assume that glass transition is a non-equilibrium phenomenon. However, there is a line of reasoning based on the emergence of an 'entropy crisis' that there is an underlying 'ideal' or thermodynamic glass transition, at the so-called Kauzmann temperature for quenched systems (see e.g. [10, 11]). The glass transition for simple fluids has been shown to be relatively insensitive to the cooling or compression rates accessible in simulation [12]. Therefore for these simple fluids on simulation timescales and much longer, there should be a prospect that an 'ideal' glass can be estimated by extrapolation to $D = 0$ for densities higher than the nucleation values. The glass transition packing fraction, ζ_g, has to be located by extrapolation of the self-diffusion coefficients, D or fluidities (inverse shear viscosity, η_s) to zero for the states prior to nucleation.

2. Results and discussion

Figure 1 shows several radial distribution functions for the hard-sphere fluid on either side of the nucleation packing fraction, ζ_n. Figure 2 shows a corresponding plot for the soft-sphere fluid with $n = 5$ at states in the metastable fluid and solid branches of the phase diagram. Both systems exhibit a definite transition from a liquid-like radial distribution function to that of a crystalline or polycrystalline sample. Particle configurations for FCC and BCC are characterized by peaks in the radial distribution function (in units of the position of the first peak): 1.0, 1.4, 1.7 and 2.0 for FCC, and 1.0, 1.1, 1.6 and 2.0 for BCC. The hard-sphere system appears to be nucleating into an FCC form whereas because of the broadness of the peaks in the plot in figure 2, it is not certain what crystalline form the r^{-5} system is adopting, although one would expect it

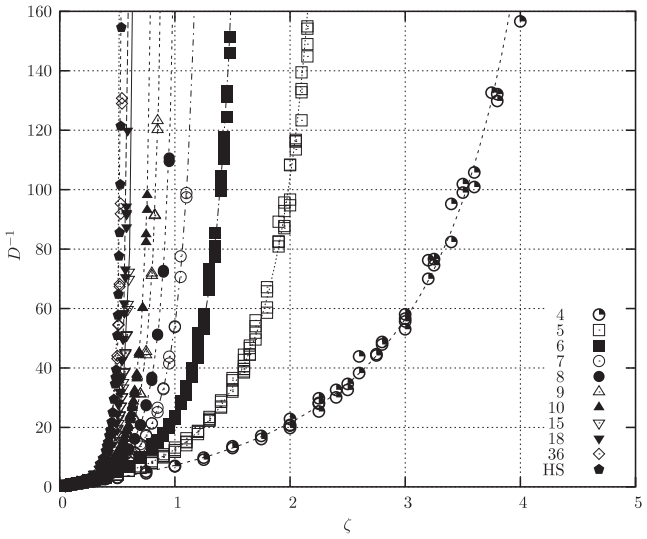

Figure 3. The inverse self-diffusion coefficient, D^{-1} against the packing fraction $\zeta = \pi N\sigma^3/6V$ for various n values (given on the figure), with $N = 2048$. D is in units of $\sigma(\epsilon/m)^{1/2}$ where σ and ϵ are the potential parameters from equation (1). The curves are the predictions of the fit formula given in equation (3) with $m = 2$ for self-diffusion coefficients in the range $0.005 < D < 1.0$.

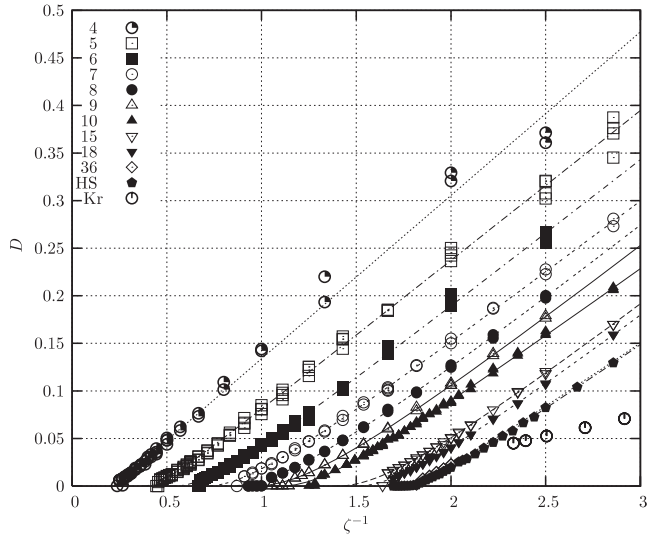

Figure 4. D against ζ^{-1}, where the lines are least square fits to the diffusion coefficient data in the range $0.005 < D < 1.0$ using equation (3) with $m = 2$. Fluidity, η_s^{-1} data for supercritical krypton at 298 K, taken from [35], are also shown on the figure. The effective packing fraction was calculated from the Lennard-Jones potential σ for Kr (= 0.3633 nm) [36]. The viscosity, η_s, is in units of 10^{-5} Pa s.

to be BCC for such a soft-potential [13]. Nucleation of soft-sphere fluids (with $n = 12$) has also been simulated on an MD timescale elsewhere [14].

The simulation data and associated statistics are given in supplementary files[3]. We concentrate discussion mainly on the self-diffusion coefficients, D, even though the same trends were exhibited with the fluidities (η_s^{-1}). The statistics are much better for D. In figure 3, curves of D^{-1} against particle packing fraction for various values of n are shown. D^{-1} increases more rapidly with particle packing fraction, and decreases with n at a given value of ζ. For large n the data converge towards the 'hard-sphere' line, with the limiting hard-sphere diameter equal to σ. In [6, 7] it was shown that a plot of D against ζ^{-1} for the soft-particle systems is linear at intermediate densities,

$$D(n,\zeta) \equiv y(n,\zeta) = a(n)\frac{1}{\zeta} - b(n), \tag{2}$$

where $a(n)$ and $b(n)$ are n-dependent constants. This general form for the density dependence of a transport coefficient dates back at least to Hildebrand [15]. The intercept value of ζ^{-1} when $D = 0$ is defined as ζ_i^{-1}, and $\zeta_i = a/b$ can be taken as an approximate value of the glass transition packing fraction, ζ_g. However, there is a departure from this trend at high packing fractions in the metastable region, as noted by Woodcock and Angell [16]. A more accurate representation of the data at high densities is given by a modification of equation (2),

$$D(n,\zeta) \equiv \frac{y^{m+1}(n,\zeta)}{c(n) + y^m(n,\zeta)} \tag{3}$$

where m is an integer and $c(n)$ is another (small) constant. This formula has the additional flexibility to achieve a better fit to the self-diffusion coefficients at high density, and hence an improved estimate for the glass transition. This is without sacrificing the linear behaviour of D on ζ^{-1} evident at intermediate packing fractions. $c(n)$ is a small positive number, and for low packing fractions the formula in equation (3) effectively reduces to that in equation (2). At higher packing fractions close to the glass transition, the new formula gives a value of D higher than equation (2), which is consistent with the simulation date (see figure 4 where D is plotted against ζ^{-1}) and experimental data on simple molecular systems [18]. By trial and error, the value $m = 2$ in equation (3) was found to be about optimum. For equation (3), the formula for the glass transition packing (i.e. when the formula in equation (3) predicts $D = 0$) is also $\zeta_i = a/b$ as for equation (2), except the non-linear least squares fit values for a and b will be different in the two cases. The fit formula of equation (3) can be seen, in figure 4, to reproduce the linear region at intermediate packing fractions *and* the high density behaviour where the simulation data falls above the extrapolated linear region. The fluidity of krypton at liquid-like densities and $T = 298$ K are also given on this figure for comparison (self-diffusion data at high pressures for simple liquids are quite rare when compared with the shear viscosity). These data show a near linear dependence of η_s^{-1} on ζ^{-1}, which is the same behaviour as for D. Further details on the experimental data are given in the caption to figure 4.

In figure 4 it may be seen that the slope, a, of the low and intermediate density regime is almost independent of n, only showing a noticeable change for the $n = 6, 5$, and 4 fluids. Consequently, the intercept, $\zeta_g^{-1} = b/a$ or the position of the glass transition is essentially determined by b. Clearly, b, decreases with softness which means that ζ_g increases with softness. A more quantitative explanation may be obtained by

[3] The supplementary files contain the potential energies per particle, self-diffusion coefficients and shear viscosities. (available at stacks.iop.org/JPhysCM/20/115102)

considering the case of hard spheres. From Enskog kinetic theory, for $\zeta \to 0$, $D \to D_B = \sqrt{\pi}/16\zeta = 0.1108/\zeta$, which is the first order approximation. The second approximation is $1.01724\sqrt{\pi}/16\zeta = 0.1127/\zeta$ and the limiting value is $1.019\sqrt{\pi}/16\zeta = 0.1129/\zeta$ [17]. In practise, there is an N-dependence to the values of these parameters on fitting to hard-sphere molecular dynamics data with equation (2), for example for $\zeta > 0.2$ this procedure gives, $a = 0.103, 0.119$ and 0.133 for $N = 32, 108$ and $109\,76$, respectively. The first order approximation is sufficiently accurate for the analytic treatment below, i.e. $a(HS) = 0.111$. A least squares fit to hard-sphere MD data taken from [5] gives for a, b, values of $0.1310(5), 0.241(1)$ and $0.1124(4), 0.230(5)$ for ζ above and below 0.2, respectively. The numbers in brackets refer to the uncertainty in the last digit. The fits used data down to packing fractions of 0.0001. Note that in the lower density regime the inverse density coefficient is within 0.5% of the kinetic theory prediction. If data in the fit is confined to values in an intermediate region, 0.05–0.35, the (a, b) parameters are $0.111, 0.181$ respectively. Therefore the value of a is very close to the expected kinetic value for data below ca. $\zeta \simeq 0.35$, but increases systematically as higher density data are included in the fit. The value of b goes through a minimum for data sets confined to an intermediate density range.

From the work of Rosenfeld and Bastea [19, 20], the density dependence of the self-diffusion coefficient has been written in terms of the excess entropy $D = D_B g(\sigma) \exp(\gamma s^{ex}/k_B)$, where D_B is Boltzmann's formula for the self-diffusion coefficient in the dilute gas phase, $g(\sigma)$ is the radial distribution function at contact, γ is a constant, s^{ex} is the excess entropy per particle and k_B is Boltzmann's constant. Now, at low densities, $g(\sigma) = (Z-1)/B_2\zeta = (B_2\zeta + B_3\zeta^2)/B_2\zeta$, where Z is the compressibility factor, and B_2 and B_3 are the second and third virial coefficients. As $s^{ex}/k_B = -(B_2\zeta + B_3\zeta^2/2 + \cdots)$ then $\exp(\gamma s^{ex}/k_B) = 1 + \gamma s^{ex}/k_B + \cdots = 1 - \gamma B_2\zeta + \cdots$. Therefore,

$$D = \frac{\sqrt{\pi}}{16\zeta} - \frac{\sqrt{\pi}}{16}(B_2\gamma - B_3/B_2) = a/\zeta - b \qquad (4)$$

where $a = \sqrt{\pi}/16 = 0.1108$, which is a little low for high density, and $b = \sqrt{\pi}(4\gamma - 2.5)/16$ taking, $B_2 = 4$ and $B_3 = 10$ [22]. Therefore to obtain the form, $D = a/\zeta - b$, it is necessary to consider the equation of state to the level of the third virial coefficient. For the adopted value of $\gamma = 0.8$, we have $b = 0.08$ which is significantly smaller than the simulation data produce. But it is already known that Bastea's formula with $\gamma = 0.8$ does not match the simulation data well at low density (see figure 1 in [20]). For $\gamma = 1.1$, we get $b = 0.21$, which is closer to the simulation value of 0.235(5). Even though the MD data presented as D against ζ^{-1} in relative terms exposes mainly the lower density behaviour, the low density expansion predicted from equation (4) represents the simulation data reasonably well in the intermediate density region and at even higher densities, depending on the accuracy required.

Turning now to the soft-sphere particles, taking all the data points, *linear* fits to D against ζ^{-1}, give a and b values as a function of the potential exponent, n. The parameter, a increases with softness. Taking the self-diffusion coefficient data for less then half the density of the fluid at the fluid–solid coexistence, a has values of $0.139, 0.129, 0.124, 0.122, 0.120$ and 0.116 for $n = 4, 5, 6, 8, 10$ and 12, respectively. Taking all the fluid data, these numbers increase slightly to $0.142, 0.131, 0.126, 0.124, 0.122$ and 0.121. In the $\zeta \to 0$ limit, the first order solution from kinetic theory is [17, 19],

$$D = \frac{\sqrt{\pi}}{16\zeta}\left(\frac{2k_BT}{mn\epsilon}\right)^{2/n}\frac{1}{A_1(n)\Gamma(3-2/n)} \qquad (5)$$

where m is the mass of the molecule, which goes over to the hard-sphere kinetic theory solution as $n \to \infty$. (In passing we note that there is a misprint in table 3 of [19]; the column headings A_1 and A_2 should be reversed. The original data are in [17], p. 172.) It is reasonable to use the same analytic form for the self-diffusion coefficient, $D = aZ/B_2\zeta^2 \exp(\gamma s^{ex}/k_B)$, for the soft spheres as for the hard spheres, where now the quantities in the formula refer to those for soft spheres. Expanding this we get, again, $D = a/\zeta - b + \cdots$. It can be seen from figure 4 that the coefficient a is only weakly dependent on n. The first order kinetic theory value from [17] is 0.1108 for $n \to \infty$ and 0.1397 for $n = 4$, which is in good agreement with the simulation value (0.139). The expansion gives, $b = a(\gamma B_2(1 - 3/n) - B_3/B_2)$, which increases with n, as is found from the simulation (note that all quantities are n-dependent now).

In the simulations nucleation was found to occur when the diffusion coefficient became less than about 0.005, for all n. Consequently, the glass transition temperature from the simulation was estimated as the value of ζ at which $D \to 0$, extrapolating the self-diffusion coefficient data from below ζ_n. Figure 5 shows these data fitted by equation (3) with $m = 2$ in the small-D regime (and this route to the glass transition is called 'I'). The estimated value of the glass transition does depend on the formula used to extrapolate the simulation data

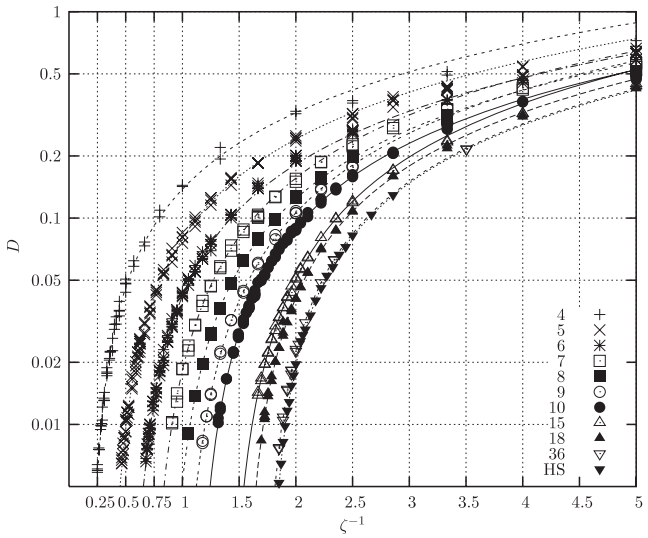

Figure 5. D against ζ^{-1}. Note that D is given on a log scale. The diffusion coefficient data were fitted in the range $0.005 < D < 0.1$, using equation (3) with $m = 2$.

Table 1. Packing fractions and their ratios for variable n. Key: n, the soft-sphere potential exponent; ζ_f, the packing fraction of the fluid phase at coexistence; ζ_s, the packing fraction of the solid phase at coexistence; ζ_n, the packing fraction at nucleation of the fluid; ζ_g, a lower bound on the packing fraction at the glass transition, estimated by extrapolation of the self-diffusion coefficient to zero according to $D = a/\zeta - b$ fitted in the range $0.005 < D < 0.02$. The coexistence packing fractions for the various n were obtained by least squares fitting to a polynomial the coexistence data of Agrawal and Kofke [3, 4]. $\zeta_{g,fH} = \zeta_f(3/2)^{3/n}$ is the prediction of the Hunt expression using the hard-sphere fluid as the coexistence reference, and $\zeta_{g,sH} = \zeta_s(3/2)^{3/n}$ is the corresponding value using the hard-sphere solid. The bracket after the ζ_g value for $n = 4$ and 5 refers to the statistical uncertainty in the last digit.

n	ζ_f	ζ_s	ζ_n	ζ_g	ζ_s/ζ_f	ζ_n/ζ_f	ζ_g/ζ_f	ζ_n/ζ_s	$\zeta_{g,fH}$	$\zeta_{g,sH}$
4	2.98	3.00	4.1	4.8(1)	1.005	1.37	1.60	1.37	4.05	4.06
5	1.73	1.74	2.2	2.5(1)	1.008	1.27	1.44	1.26	2.21	2.22
6	1.22	1.23	1.5	1.66	1.012	1.23	1.36	1.22	1.49	1.51
7	0.967	0.983	1.15	1.25	1.016	1.19	1.29	1.17	1.15	1.17
8	0.826	0.843	0.975	1.06	1.021	1.18	1.28	1.28	0.96	0.98
9	0.738	0.757	0.860	0.93	1.025	1.17	1.27	1.27	0.84	0.87
10	0.680	0.700	0.78	0.84	1.029	1.15	1.24	1.12	0.77	0.79
12	0.610	0.633	0.671	0.74	1.037	1.10	1.21	1.06	0.68	0.70
15	0.558	0.585	0.605	0.66	1.048	1.08	1.18	1.03	0.61	0.63
18	0.531	0.562	0.595	0.62	1.056	1.12	1.17	1.06	0.57	0.60
36	0.493	0.534	0.555	0.56	1.084	1.13	1.15	1.04	0.51	0.55
72	0.488	0.535	0.525	0.54	1.097	1.08	1.11	0.98	0.49	0.54
288	0.491	0.542	0.53	0.54	1.104	1.08	1.11	0.98	0.49	0.54
HS	0.493	0.545	0.545	0.55	1.105	1.105	1.12	1.00	—	—

to $D \to 0$, especially as n decreases, and the nucleation and glass transition packing fractions move to densities which, in relative terms, are further into the solid phase density regime. Another formula which also fits the $D(\zeta)$ data well in the low D regime is $D = a_1(\zeta^{-1} - a_2)^{a_3}$ where a_1, a_2 and a_3 are empirical constants. Note this formula has the wrong density dependence as $\zeta \to 0$, so it is only applicable for small values of D close to freezing, and should be treated as empirical only. This equation was inspired by the formula used to extrapolate D to the mode coupling temperature, where we have replaced T by ζ^{-1} [21]. We call this formula to obtain ζ_g, route 'II'. There is not a rigorous formula, and in fact there is no apparent concensus about the analytic form for $D(\zeta)$ close to ζ_g. We have discussed above, for ζ close to the freezing or glass transition, that D is not linear in ζ^{-1}. Because of the curvature of this function, a linear extrapolation against ζ^{-1} in the smallest D value range provides a lower bound on the value of ζ_g (a procedure we refer to as route 'III'). Using D values in the range 0.005–0.02, then for $n = 4$ the estimates of ζ_g by routes I, II and III are, 14.8, 3.9 and 4.8, respectively for the $N = 2048$ data. The corresponding values for $n = 5$ are, 2.9, 2.66 and 2.50. It is the route 'III' values that are given in table 1.

The nucleation and glass transition packing fractions obtained by procedure III are compared with the coexistence values in table 1. The glass transition for $n = 12$ of 0.74 (table 1) agrees very well with previous simulation estimates of 0.75 ± 0.05 [23] and 0.79 ± 0.05 [24], also based on linear extrapolations to zero D. For hard spheres the glass transition has been variously estimated to be between 0.57–0.58 (e.g. see [25]). Using extrapolation formulae I, II and III, values of 0.580, 0.569 and 0.555, are obtained. The estimated glass transitions using the fluidity, η_s^{-1}, where η_s is the shear viscosity, rather than D give values for ζ_g which are typically within ca. 5% of the values obtained from D. The scatter is greater than for the self-diffusion derived numbers however, as the shear viscosity is a collective property whereas the self-diffusion coefficient is a single particle property with $\sqrt{N}$ better statistics.

For all n, both the nucleation and glass packing fractions are in general found at densities greater than the coexisting fluid and solid densities. Relative to the freezing point densities, these two points move further into the solid part of the phase diagram as the interaction becomes softer. For example, for $n = 4$, solid coexistence packing fraction is 3.00, and it nucleates at $\zeta = 4.1$ and the glass transition is estimated to be at a minimum, 4.8. In two cases, $n = 72$ and $n = 288$, nucleation occurred at a density in between the equilibrium coexisting densities of fluid and solid. Cardenas and Tosi [26] located the glass transition in soft-sphere systems with a mean-field approach based on a replica-symmetry breaking method. They also found that the glass transition lay increasingly further within the solid phase with increasing softness, although for the range of n covered, their values are larger than those determined here. For $n = 4, 6, 9$ and 12 it was predicted in [26] that $\zeta_g = 15, 3.5, 1.5$ and 1.1, compared with $\geqslant 4.8$, $\geqslant 1.66$, $\geqslant 0.93$ and $\geqslant 0.74$ obtained in this study, respectively. From the work of Agraval and Kofke [3, 4], the freezing packing fractions of the inverse power fluids are smooth and quite regular as a function of n^{-1} and well-represented by a polynomial. However, this is not a monotonic function, and has a minimum at about $n = 72$. One might expect a similar trend for the nucleation packing fraction ζ_n. Both functions have similar shapes and ζ_n can roughly be viewed as ζ_f shifted upwards. However, the shift is not uniform and the amount of the shift depends on the softness. Also note, that the ζ_n show more scatter around the average trend for ζ_f, as one would expect for a non-equilibrium event, and the simulations were carried out at finite intervals of packing fraction, which limits the resolution of ζ_n. Nevertheless from the simulation data, it may be concluded that for $n > 10$ the

Table 2. The parameters for the dependence of the self-diffusion coefficient on extent of compression, on the assumption that $D(X) = D_{0,X}\exp(-\alpha_X X)$. The parameters are determined close to and just higher than the coexistence fluid density. The symbol, X, is either packing fraction, ζ, pressure P or compressibility factor, Z.

n	$-\ln(D_{0,\zeta})$	α_ζ	$-\ln(D_{0,P})$	α_P	$-\ln(D_{0,Z})$	α_Z
4	0.821	1.08	2.072	0.002 74	1.274	0.0243
5	0.363	2.13	1.814	0.009 75	1.156	0.0449
6	−0.048	3.30	1.727	0.0198	1.099	0.0626
7	−0.253	4.24	1.519	0.0351	0.984	0.0814
8	−0.561	5.29	1.547	0.0462	0.994	0.0938
9	−0.903	6.41	1.527	0.0577	0.975	0.106
10	−0.882	6.70	1.484	0.0741	0.947	0.119
12	−1.051	7.78	1.349	0.0997	0.856	0.142
15	−1.320	8.85	1.294	0.125	0.785	0.163
18	−1.755	10.29	1.283	0.141	0.754	0.179

ratio is about 1.1 and for $n < 10$ increases considerably, which might indicate a change in the nucleation mechanism.

A simple connection between the melting temperature, T_m, and the glass transition temperature, T_g was proposed by Hunt [27], that $T_\mathrm{g} \simeq 2T_\mathrm{m}/3$. If we take advantage of the density–temperature scaling unique to the soft-sphere system [7], this translates into $\zeta_\mathrm{g} \equiv \zeta_{\mathrm{g},fH} = \zeta_\mathrm{f}(3/2)^{3/n}$, or $\zeta_\mathrm{g} \equiv \zeta_{\mathrm{g},sH} = \zeta_\mathrm{s}(3/2)^{3/n}$, depending on whether one scales according to the density of the coexisting fluid or solid, respectively. These quantities are given as the last two columns in table 1. These ratios actually agree quite well with the nucleation packing fractions, ζ_n, across the softness range, rather than the estimated glass transition density. The value based on the packing fraction of the solid at coexistence gives the slightly better overall agreement with ζ_n.

For liquids under compression, the coefficient, α_D is often used to characterize the sensitivity of the self-diffusion coefficient to pressure, on the assumption that $D(P) = D_{0,P}\exp(-\alpha_P)$ (e.g. see [28]). Corresponding dependencies on the packing fraction, ζ and the compressibility factor, $Z = P/\rho T$, where ρ is the number density, can be defined. In the two latter cases, α_Z and α_ζ are the relevant quantities. A plot of $\ln(D^{-1})$ against Z, for example, for the various n values states is shown in figure 6. For the softer particles it is evident from the near linearity of the data with Z at high pressure (density) that α_Z is reasonably constant over a wide range of the compressed metastable fluid state not too far from the coexistence density, ζ_f. These data for a range of n are presented in table 2. All three definitions of α show a gradual increase in magnitude with stiffness, and in the hard-sphere limit, α_ζ, α_P and α_Z have values of ca. 12, 0.22 and 0.25, respectively. These trends are consistent with expectations that the diffusion coefficient of soft particles decreases less with increasing pressure than hard particles. We cannot get close enough to the glass transition in our simulations to test satisfactorily the often-used Doolittle equation, $D = D_0\exp(-\alpha_\zeta\zeta/(\zeta_\mathrm{g} - \zeta))$, for example [1].

A simple relationship between the self-diffusion coefficient and the shear viscosity is the well-known Stokes–Einstein, SE, relationship,

$$lD\eta_\mathrm{s} = \frac{k_\mathrm{B}T}{c\pi}, \tag{6}$$

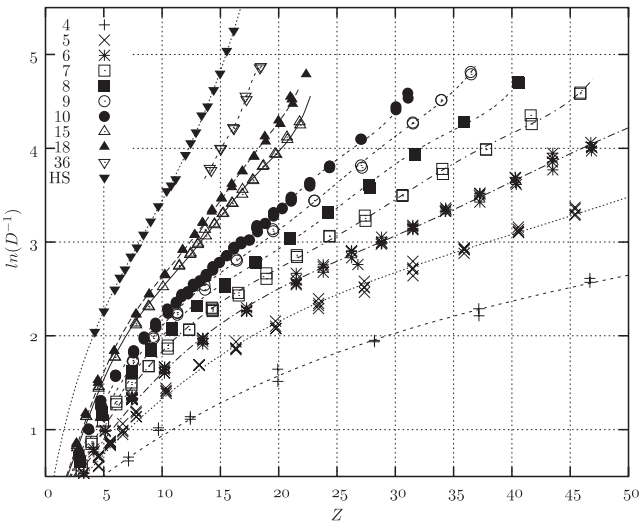

Figure 6. $\ln(D^{-1})$ against the interaction part of the compressibility factor, Z. The lines on the figure are polynomial fits to the data up to $\mathrm{O}(Z^6)$. None of the state points shown have nucleated.

where l is a characteristic diameter of the molecule, and $c = 3$ and 2, for 'stick' and 'slip' boundary conditions, respectively. Although SE strictly only applies to macroscopic spheres in a Newtonian liquid (in this limit, l is the actual diameter of the sphere), it has been tested for dense liquids and found to work remarkably well on the molecular scale with some flexibility in assigment of the molecular diameter, l or alternatively choice of the value of the c parameter (see e.g. [29] p. 262). The optimum value of c is usually found to be in between the stick and slip limits, depending somewhat on state point [30]. The main problem in applying SE to simple molecular fluids is in choosing the value of l, for which there is no rigorous prescription, especially for the very soft particles that are considered here. There is a modified SE expression due to Zwanzig, $D\eta_\mathrm{s}/\rho^{1/3} = k_\mathrm{B}T/c\pi$ [31, 32], where $\rho = N\sigma^3/V$ for N particles in volume V, which is consistent with equation (6) if $l \propto \rho^{-1/3}$. Figure 7 compares the values of c as a function of ζ and n using the definitions $l = \sigma$ and $l = \rho^{-1/3}$, respectively. The latter definition gives a more constant value of c with ζ and n in the soft-particle limit, which is closer to the slip value of 2. Even in this case, there is a gradual, but relatively small, decrease in the value

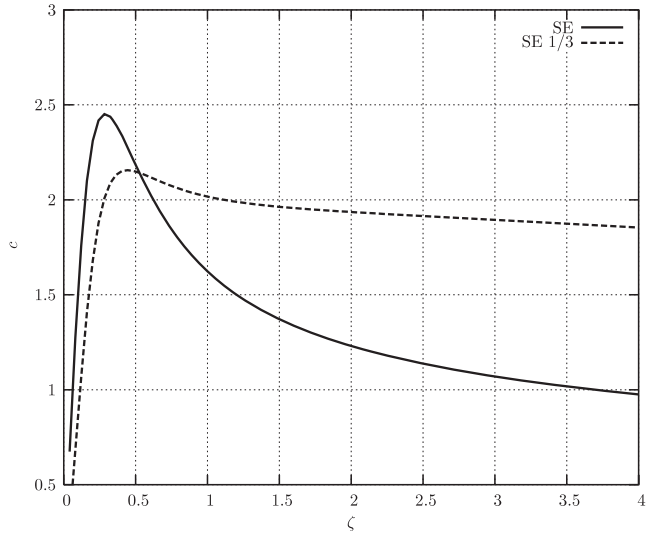

Figure 7. Test of the Stokes–Einstein coefficient, c, against ζ for the set of data for different n values. Key: (a) 'SE' is where the length scale, l in equation (6) is set to the potential characteristic distance, σ. The curve is a least squares fit to the data from $n = 4$ to 36 using the function $c = (a\zeta^b + c\zeta^d)/(1 + e\zeta^f + g\zeta^h)$ where a–h are the fit parameters. Data for smaller n values are further to the right. (b) 'SE 1/3', as for (a) except that the length scale, $l = \rho^{-1/3}$ in equation (6).

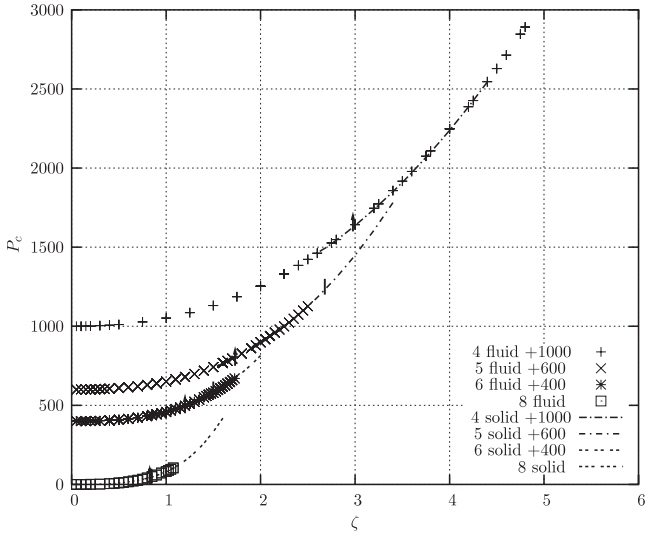

Figure 8. The configurational part of the pressure, P_c, against packing fraction, ζ for various n values which are indicated on the figure. Simulation data for the fluid state are shown as symbols, and the lines are the results of simulations carried out on FCC solid systems. The vertical bars on the figure indicate the coexisting fluid and solid densities respectively for each n value (only ζ_f for $n = 4$). The sequence of solid state simulations was carried out in order of descending density. Note the four curves are displaced vertically to different extents, by amounts given on the figure, to help distinguish the curves.

of c with increasing ζ. Nevertheless, this more constant trend associated with $l = \rho^{-1/3}$ is reasonable, as with increasing density the particles become more squashed together and the first peak in the radial distribution function moves to smaller separations. This result suggests that for very soft particles the static properties are dominated by a characteristic lengthscale (i.e. l here) that is weakly n-dependent but strongly density dependent. l is proportional to $\sim \rho^{-1/3}$, rather than the σ parameter of the potential as is found close to the hard-sphere limit. That a bulk property, the average density of the system, can be used to determine the lengthscale underpinning a molecular property (i.e. self-diffusion and shear viscosity) suggests that the precise location of the particles is of less importance for soft particles than for particles close to the hard-sphere limit. In this limit there are so many particles that interact with a given particle with an energy which is a signifcant fraction of k_BT that their precise location in space becomes less important than for particles in the large-n limit. This is illustrated in another way, in figure 8, which shows the configurational part of the pressure plotted against ζ for fluid and crystalline states. For $n = 4$–8 it may be seen that the fluid and solid state data superimpose very well at densities within the fluid–solid coexistence region and above.

3. Conclusions

Whether hard spheres and the present soft-sphere systems can be produced on a computer in a truly glassy state is still open to debate, as the present monodisperse systems nucleate in the crystalline form before these states are actually achieved. Nevertheless, the 'glassy' density obtained here by extrapolation for particles of different softnesses provides a limiting state for the compressed fluid prior to nucleation and could be useful in the context of thermodynamic descriptions of an 'ideal' glass. The work also shows that the pressure dependence of the self-diffusion coefficient or viscosity is a convenient measure of the effective softness of the molecules. In modern terminology, the soft particles could to be said to form 'strong' glasses whereas the hard sphere is a 'fragile' limit of the soft-sphere fluid [33]. (A large fragility reflects a structured potential energy landscape and the dominance of thermally activated processes, [34].) It is shown that the characteristic length scale for $n \to 4$, is determined by the average density which is only weakly dependent on n and depends mainly on the density. The potential energy landscape for these systems is sufficiently 'shallow' and featureless (due to the many interacting particles with a given particle) that the static properties of these fluids could be well-described by mean-field formulae or lattice models (see figure 8 and the accompanying discussion). An improvement is made to the Hildebrand formula for the density dependence of the self-diffusion coefficient and fluidity (inverse shear viscosity), which was shown previously to represent well these quantities for particles in the softness range considered here at intermediate densities [6]. The new formula (in equation (3)) fits the transport coefficients at the highest densities accessible (prior to nucleation). However, the good fit from that analytic form was not unique and the estimated value of the glass transition packing fraction was found to depend on the formula used to perform the extrapolation to zero diffusion coefficient. An estimate is made of a lower bound on these values for the different potential exponents, n. With increasing softness

the glass transition moves further within the solid part of the phase diagram, as predicted by Cardenas and Tosi [26], but (probably) not quite to the same extent.

Acknowledgments

The authors would like to thank the Royal Society (London) and the Polish Academy of Sciences for partly funding this collaboration. The work has been partially supported by the Polish Ministry of Science and Higher Education grant N20207032/1512 (2007–2010). We thank the referees for helpful suggestions.

References

[1] Drozd-Rsoska A, Rzoska S J, Paluch M, Imre A R and Roland C M 2007 *J. Chem. Phys.* **126** 164504
[2] Jonas J and Lee Y T 1991 *J. Phys.: Condens. Matter* **3** 305
[3] Agrawal R and Kofke D A 1995 *Phys. Rev. Lett.* **74** 122
[4] Agrawal R and Kofke D A 1995 *Mol. Phys.* **85** 23
[5] Heyes D M, Cass M J, Powles J G and Evans W A B 2007 *J. Phys. Chem.* B **111** 1455
[6] Heyes D M and Brańka A C 2005 *J. Chem. Phys.* **122** 234504
[7] Heyes D M and Brańka A C 2005 *Mol. Simul.* **31** 945
[8] Heyes D M 1997 *The Liquid State* (Chichester: Wiley) p 207
[9] Shumway S L, Clarke A S and Jónsson H 1995 *J. Chem. Phys.* **102** 1796
[10] López de Haro M and and Robles M 2006 *Physica* A **372** 307
[11] Parisi G and Zamponi F 2005 *J. Chem. Phys.* **123** 144501
[12] Speedy R J 1994 *Mol. Phys.* **83** 591
[13] Hoover W G, Young D A and Grover R 1972 *J. Chem. Phys.* **56** 2207
[14] Cape J N, Finney J L and Woodcock L V 1981 *J. Chem. Phys.* **75** 2366
[15] Hildebrand J H and Lamoreaux R H 1972 *Proc. Natl Acad. Sci.* **69** 3428
[16] Woodcock L V and Angell C A 1981 *Phys. Rev. Lett.* **47** 1129
[17] Chapman S and Cowling T G 1970 *The Mathematical Theory of Non-Uniform Gases* (Cambridge: Cambridge University Press)
[18] van Loef J J 1982 *Physica* B & C **114** 345
[19] Rosenfeld Y 1999 *J. Phys.: Condens. Matter* **11** 5415
[20] Bastea S 2004 *Phys. Rev. Lett.* **93** 199603
[21] Giovambattista N, Buldyrev S V, Starr F W and Stanley H E 2003 *Phys. Rev. Lett.* **90** 085506
[22] Hansen J P and McDonald I R 2005 *Theory of Simple Liquids* 3rd edn (Amsterdam: Academic)
[23] Cape J N and Woodcock L V 1980 *J. Chem. Phys.* **72** 976
[24] Hiwatari Y 1980 *J. Phys. C: Solid State Phys.* **13** 5899
[25] Woodcock L V 1981 *Ann. New York Acad. Sci.* **371** 274
[26] Cardenas M and Tosi M P 2005 *Phys. Lett.* A **336** 423
[27] Hunt A 1992 *J. Phys.: Condens. Matter* **4** L429
[28] Spikes H A 1990 *ASME Tribol. Trans.* **33** 140
[29] Balucani U and Zoppi M 1994 *Dynamics of the Liquid State* (Oxford: Clarendon)
[30] Heyes D M and Brańka A C 2005 *Phys. Chem. Chem. Phys.* **7** 1220
[31] Zwanzig R 1983 *J. Chem. Phys.* **79** 4507
[32] March N H and Alonso J A 2006 *Phys. Rev.* E **73** 032201
[33] Angell C A 1995 *Proc. Natl Acad. Sci.* **92** 6675
[34] Casalini R and Rolans C M 2005 *Phys. Rev.* E **72** 031503
[35] Trappeniers N J, Botzen A, van Oosten J and van den Berg H R 1965 *Physica* **31** 945
[36] Zhdanov E R and Fakhretdinov I A 2005 *J. Mol. Liq.* **120** 51